MIRROR ABERRATIONS IN A LOW GAIN FEL OSCILLATOR*

P.J.M. van der Slot[#,a], H.P. Freund[b], R. van der Meer[a], K.J. Boller[a],
[a]Mesa+ Institute for Nanotechnology, University of Twente, Enschede, The Netherlands, [b]Science Applications International Corp., McLean, VA 22102, U.S.A.

Abstract

To generate radiation with high spatial - and temporal quality in free-electron lasers (FELs), oscillators are to be used which are based on the combination of low gain with a large number of roundtrips in a low-loss optical resonator. Clearly, in this situation any additional loss or aberration may seriously degrade the performance and beam quality, and this becomes extremely important for high average power FEL oscillators. Nevertheless, so far no systematic study has been made how various mirror aberrations affect the performance of such low gain FEL oscillators. Here we present the first results of such a study. The approach is based on the optical propagation code OPC with GENESIS 1.3 and MEDUSA as gain codes.

INTRODUCTION

In a low-gain free-electron laser (FEL), the gain is not sufficient to saturate the laser in a single pass. Mirrors are used to form an optical cavity around the gain section and when the single pass gain minus the total roundtrip loss is positive the optical field will start to grow. When this happens a bright, highly directional and highly coherent output beam can be produced by extracting part of the optical field from the cavity, usually by making one of the mirrors partially transmitting. It is well known that aberrations, either produced in the gain section or by the mirrors can significantly reduce the performance of the laser oscillator [1]. For example, thermal distortion of the outcoupler is one of the major limiting factors to push the output of high-power FELs to higher levels [2]. Mirrors are usually not ideal and may posses various types of aberrations: spherical, coma, astigmatism, *etc*. The type of aberrations we will be considering here result in wavefront deformation, and the aberration function can be described as a sum over Zernike polynomials, each term describing a certain type of aberration [3].

To model the FEL oscillator including mirror aberrations, we use the Optics Propagation Code (OPC) [4] for the non-amplifying part of the resonator, and the MEDUSA [5] and GENESIS 1.3 [6] codes for the gain section. OPC propagates the optical field using various methods to propagate the optical field from one optical component to another. All methods rely numerically on fast discrete Fourier transforms. Currently, the optical components available are mirrors, lenses, phase masks, and round and rectangular diaphragms. OPC also includes Zernike polynomials to describe various types of mirror aberrations. It can interface with two FEL gain models, MEDUSA and GENESIS 1.3.

MEDUSA is a three-dimensional simulation code that includes time-dependence, harmonics, and start-up from noise. It models electron beam transport elements, helical and planar wigglers, and the optical field is a superposition of Gaussian modes. Electron trajectories are integrated using the three-dimensional Lorentz force equations in the combined magnetostatic and optical fields. No wiggler average orbit analysis is used.

GENESIS 1.3 is also a three-dimensional simulation code that includes time-dependence, harmonics and start-up from noise, although the latter is only available for time-dependent simulations. It also models electron beam transport elements, and helical and linear wigglers. However, it applies a wiggler average to the electron trajectories, and the transverse profile of the optical field is discretized on uniformly spaced Cartesian grid and numerically propagated.

To model an FEL oscillator, one typically starts with the FEL gain code (MEDUSA or GENESIS 1.3) to determine the optical field at the wiggler's exit after the first pass. The complex optical field amplitude is written to a file, which is then read by OPC and propagated to the downstream mirror, which is partially transmitting in the example we are considering. The portion of the optical field that is reflected is then propagated to the upstream mirror (which is a high reflector) by OPC, and then back to the wiggler entrance. The field at the wiggler entrance is then reduced to an ensemble of Gaussian modes that is used as input for MEDUSA, or is directly used by GENESIS 1.3 for the next pass. This process is repeated for an arbitrary number of passes.

In the remaining part we will first describe the aberration-free FEL oscillator and then present the behaviour of the FEL oscillator when spherical mirror aberrations are included using both MEDUSA and GENESIS 1.3 to model the gain section. We will discuss the case where the aberrations are only applied to the outcoupler and the case where the same aberration is applied to both mirrors.

LOW GAIN FEL OSCILLATOR

As a test case we will consider a low gain FEL oscillator with a partially transmitting outcoupler. The main system parameters are summarized in Table 1. The FEL consist of a linear wiggler with equal focussing in both directions and consists of 52 periods. For the simulations with MEDUSA a taper consisting of one period is added on both sides of the wiggler for proper injection and extraction of the electron beam, bringing the total number of periods to 54. To limit the computational time, we present the results of steady-state simulations.

*Work supported in part by the Office of Naval Research (HPF).
#p.j.m.vanderslot@utwente.nl

Table 1: FEL System Parameters

Parameter	Symbol	Value	Unit
Beam energy	E_b	16.8	MeV
Energy spread (rms)	$\delta E_b/E_b$	0.9	%
Peak current	I_b	35	A
Normalized emittance	$\varepsilon_{n,x}$ $\varepsilon_{n,y}$	40	μrad
Beam radius	R_b	0.651	mm
Wiggler parameter	K	0.7	(rms)
Wiggler period	λ_w	3.3	cm
Number of periods	N_w	52	
Radiation wavelength	λ	22	μm
Resonator length	L_c	7.1979	m
Rayleigh length	z_R	1.00	m
Radius of curvature	R_c	3.877	m
Transmission outcoupler	T_c	1.8	%
Mirror loss	α_m	0.6	%
Mirror radii	R_m	60	mm

For the parameters of Table 1, Fig. 1 shows the steady-state, single-pass gain as predicted by MEDUSA and GENESIS 1.3 as a function of the kinetic electron beam E_b. Both codes predict a maximum gain for E_b=16.8 MeV for λ=22 μm, however, the gain predicted by MEDUSA is about 15 % higher. Still the agreement between the two codes is very reasonable. In the remaining part of the paper the two codes use the respective electron beam energy that produces maximum single pass gain.

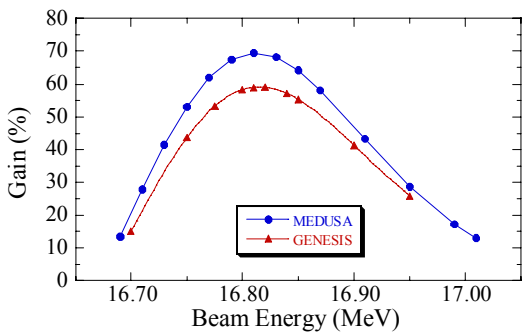

Figure 1: Steady-state single pass gain as a function of beam energy.

The main parameters for the resonator are also given in Table 1. The transmission of the outcoupler is 1.8 % and the both mirrors have a loss of 0.6 %. The total roundtrip loss is therefore 3 %. The oscillator has therefore ample gain to be above threshold. As GENESIS 1.3 cannot start from noise for steady-state simulations, both codes are initialized with a seed power equal to 1 μW. This power should be sufficiently close to the noise power in the system to study the start-up phase of the oscillator when aberrations are present. The intracavity power at the wiggler's exit and gain are shown in Fig. 2 as a function of the pass number for an aberration-free oscillator. After 200 passes, the saturated intracavity power is equal to 74 MW and 65 MW for GENESIS 1.3 and MEDUSA respectively. Agreement between the two codes is very good except that MEDUSA predicts pass-to-pass oscillations while GENESIS 1.3 does not. This oscillation arises in MEDUSA due to the higher gain and consequent guiding of the mode within the wiggler [7,8]. The MEDUSA code predicts fewer passes for reaching saturation than GENESIS 1.3 due to the higher single-pass gain observed in MEDUSA.

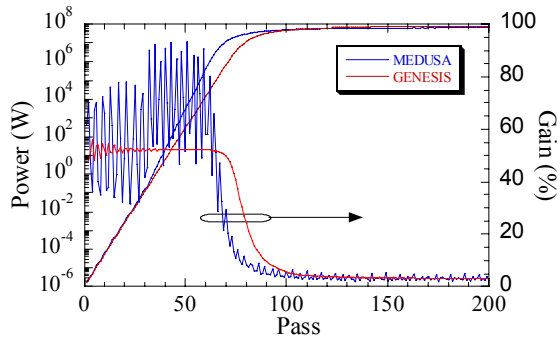

Figure 2: Intracavity power at wiggler's exit and gain versus pass number. No aberrations.

The rms spot radius of the optical mode on both the down- and upstream mirror is shown in Fig. 3. Again, agreement between the two codes is very good except that MEDUSA predicts pass-to-pass oscillations while GENESIS 1.3 does not. The oscillation in the gain that can be observed in Fig. 2 is linked to the oscillation in the rms spot radius. We also observe that the higher gain between passes 30 and 70 found with MEDUSA is associated with a smaller rms spot radius on the upstream mirror. Both MEDUSA and GENESIS 1.3 predict a slight

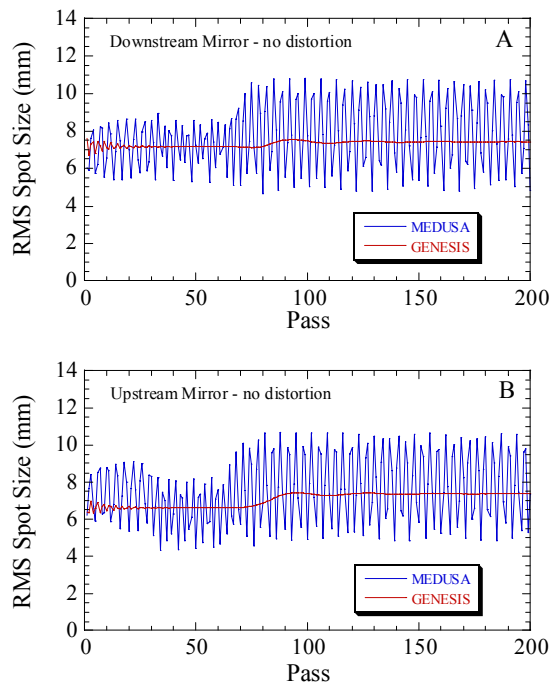

Figure 3: Rms spot size of the optical mode on the down- (A) and upstream (B) mirror. No aberrations.

increase in the rms spot radius on both mirrors when the oscillator saturates. GENESIS 1.3 (MEDUSA) predicts an equal rms spot radius of 7.4 mm (8.1 mm, averaged over last 100 passes) at both mirrors when the oscillator is saturated, while initially the spot radius on the downstream mirror is somewhat larger (smaller) than on the upstream mirror.

SPHERICAL ABERRATIONS

Now that the performance of the aberration-free oscillator has been discussed we will apply a spherical aberration to the downstream mirror first. The aberration function Φ used is given by [3]

$$\Phi = \frac{\delta a}{\lambda}\left(6\rho^4 - 6\rho^2 + 1\right) \qquad (1)$$

where δa is the aberration amplitude, λ is the radiation wavelength and $\rho = r/R_m$, with r the radial coordinate and R_m the mirror radius. Note that this aberration function when applied to a curved mirror will produce the same intensity profile in the image plane as for a $\Phi = 6\delta a\rho^4/\lambda$ aberration except for a small longitudinal displacement [3].

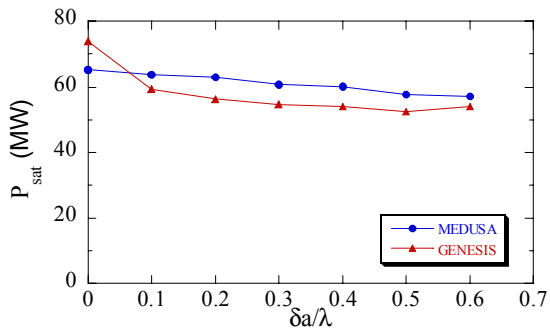

Figure 4: Saturated power at the wiggler's exit versus $\delta a/\lambda$ for the aberration applied to the downstream mirror.

The saturated power P_{sat} at the wiggler's exit is plotted in Fig. 4 as a function of the normalized aberration amplitude $\delta a/\lambda$. MEDUSA predicts a very gradual decrease from 65 to 57 MW when $\delta a/\lambda$ is increased from 0 to 0.6, while GENESIS 1.3 predicts a more pronounced initial decrease before it levels of. Again the codes predict very similar performance. The corresponding rms spot radius on both mirrors is shown in Fig. 5 versus the pass number for $\delta a/\lambda$=0.30. In contrast to the aberration-free oscillator, GENESIS 1.3 now predicts a slight decrease (increase) in spot radius at the down(up)stream mirror when the laser saturates. MEDUSA, on the other hand, predicts a slight increase in spot radius on the downstream mirror while it is approximately constant on the upstream mirror. GENESIS 1.3 predicts an rms spot radius of 6.7 (6.0) mm at the down(up)stream mirror, which is less than it would be for an aberration-free resonator and it indicates an asymmetric intracavity field distribution when the oscillator is saturated. The corresponding numbers for MEDUSA (averaged over the last 100 passes) are 7.2 (6.6) mm, showing slightly larger spots compared to GENESIS 1.3.

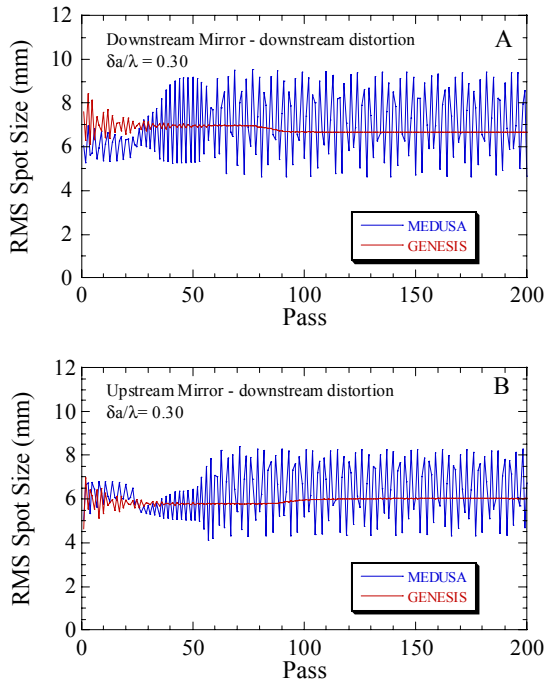

Figure 5: RMS spot radius at the down- (A) and upstream (B) mirror versus pass number for $\delta a/\lambda$=0.30. Aberration is applied to downstream mirror alone.

For the case of both mirrors having the same spherical aberration (Eq. 1), Fig. 6 shows the saturated power at the wiggler exit as a function of $\delta a/\lambda$. GENESIS 1.3 predicts the same power level compared to the case of only a distorted downstream mirror (Fig. 4) up to $\delta a/\lambda$=0.3. For $\delta a/\lambda$ = 0.325 no steady state is reached and the power oscillates over a range indicated by the error bar in Fig. 6 after 1000 roundtrips. For all other values investigated, a steady state is reach within 200 roundtrips. For $\delta a/\lambda$=0.35, P_{sat} suddenly increases to 80 MW, more than obtained with the aberration-free oscillator. For larger values of the aberration amplitude P_{sat} gradually drops until it is almost equal to the value obtained with only distortion on the downstream mirror for $\delta a/\lambda$=0.6. MEDUSA shows a similar feature, though to a lesser extent and for a different $\delta a/\lambda$ (0.1). Around $\delta a/\lambda$=0.35

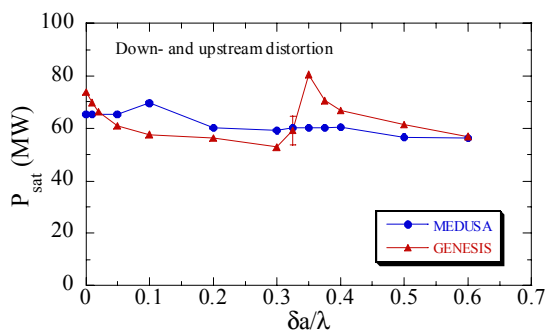

Figure 6: Saturated power at the wiggler's exit versus $\delta a/\lambda$ for the aberration applied at both mirrors.

MEDUSA seems also to predict a slightly higher P_{sat} compared to only a distorted downstream mirror.

The rms spot radius of the optical mode on both mirrors is shown in Fig. 7 as a function of the pass number for $\delta a/\lambda$=0.35. It clearly shows a different evolution of the optical mode (cf. Figs. 3 and 5). The oscillations in the spot radius on the upstream mirror have disappeared for the first 50 roundtrips (MEDUSA) while they are clearly visible for the other two cases considered here. Also the magnitude of the remaining oscillations is smaller. After a few passes, MEDUSA shows the spot radius on the downstream mirror to be smaller than on the upstream mirror and after about 25 passes this is reversed and the spot size on the downstream mirror starts to oscillate. After about 50 passes the spot size on the upstream mirror starts to oscillate as well and after about 80 passes the average spot radii becomes 6.0 mm on both mirrors when the laser saturates. GENESIS 1.3 on the other hand shows a spot radius on the downstream mirror that is (on average) larger than on the upstream mirror for all passes up to and including saturation (after about 165 passes where the gain is only 1% above the losses). In saturation, GENESIS shows a spot size of 6.4 mm on both mirrors, slightly larger than predicted by MEDUSA. Both codes produce a smaller spot on the mirrors compared to the aberration-free oscillator.

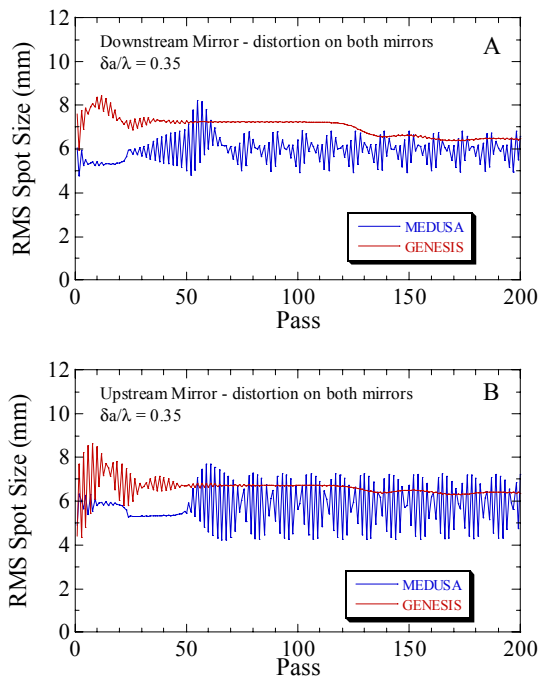

Figure 7: RMS spot radius at the down- (A) and upstream (B) mirror versus pass number for $\delta a/\lambda$=0.35. Aberration is applied to both mirrors.

DISCUSSION AND CONCLUSIONS

Apart from the difference between GENESIS 1.3 and MEDUSA regarding the oscillations in the optical mode size, we find a very good overall agreement between the oscillator performance predicted by MEDUSA and by GENESIS 1.3. Small differences can be observed, especially during the initial growth of the optical field, where the gain is still high. We believe that the observed differences between GENESIS 1.3 and MEDUSA are due to a different optical guiding [7,8] predicted by the two codes. Optical guiding will shift the waist of the optical field towards the end of the wiggler when the gain is high, *i.e.*, during the build-up phase of the oscillator. Due to the different guiding, the optical mode size is different, and indeed, the single pass gain calculations shown in Fig. 1 show the optical mode size at the wiggler exit produced by MEDUSA to be smaller than the one produced by GENESIS 1.3. This results in a different evolution of the intracavity optical field, where similar oscillations were found in simulations of short Rayleigh range oscillators [9].

Analysis of the GENESIS 1.3 data shows that with no aberrations present the FWHM of the optical field at the wiggler entrance (exit) is 4.4 (3.5) mm when the gain is high and changes to 3.9 (5.7) mm when the laser saturates. With aberration only applied to the downstream mirror this changes into 3.4 (4.6) and 3.9 (4.9) mm respectively, while the corresponding data for aberration on both mirrors is 6.5 (2.8) and 4.9 (5.0) mm respectively. As in the latter case the spot size is almost the same on both mirrors, this leads to the conclusion that the optical field is almost symmetrical within the oscillator, contrary to the other two cases presented. Whether this is the cause for the higher saturated power in the latter case is still under investigation.

We have presented the performance of a low gain FEL oscillator when spherical aberration is applied to one or both of the mirrors. For aberration amplitudes less than half a wavelength, both MEDUSA and GENESIS 1.3 show only a minor degradation in performance, where $\lambda/2$ is a reasonable relaxed specification for the mirrors in the infrared and visible and possible also for operation in the ultra-violet wavelength range.

REFERENCES

[1] N. Hodgson and H. Weber, IEEE J. Quant. Elec. **29** 2497 (1993).
[2] G. Neil *et al.*, Nucl. Instrum. Methods Phys. Res., A**557** 9 (2006).
[3] M. Born and E. Wolf, *Principles of Optics*, Pergamon Press, Oxford (1980).
[4] J.G. Karssenberg *et al.*, J. Appl. Phys. **100**, 093106 (2006).
[5] H.P. Freund *et al.*, IEEE J. Quantum Electron. **27**, 243 (2000).
[6] S. Reiche, Nucl. Instrum. Methods Phys. Res. A**429** 243 (1999).
[7] P. Sprangle *et al.*, Phys. Rev. A **36** 2773 (1987).
[8] E.T. Scharlemann *et al.*, Phys. Rev. Lett. **54** 1925 (1985).
[9] P.P. Crooker *et al.*, Phys. Rev. ST-AB **8** 040703 (2005).